Vol 463|4 February 2010|doi:10.1038/nature08755

LETTERS

Migrating tremors illuminate complex deformation beneath the seismogenic San Andreas fault

David R. Shelly[1]

The San Andreas fault is one of the most extensively studied faults in the world, yet its physical character and deformation mode beneath the relatively shallow earthquake-generating portion remain largely unconstrained. Tectonic 'non-volcanic' tremor, a recently discovered seismic signal[1] probably generated by shear slip on the deep extension of some major faults[2–4], can provide new insight into the deep fate of such faults, including that of the San Andreas fault near Parkfield, California[5]. Here I examine continuous seismic data from mid-2001 to 2008, identifying tremor and decomposing the signal into different families of activity based on the shape and timing of the waveforms at multiple stations[6]. This approach allows differentiation between activities from nearby patches of the deep fault and begins to unveil rich and complex patterns of tremor occurrence. I find that tremor exhibits nearly continuous migration, with the most extensive episodes propagating more than 20 kilometres along fault strike at rates of 15–80 kilometres per hour. This suggests that the San Andreas fault remains a localized through-going structure, at least to the base of the crust, in this area. Tremor rates and recurrence behaviour changed markedly in the wake of the 2004 magnitude-6.0 Parkfield earthquake[6,7], but these changes were far from uniform within the tremor zone, probably reflecting heterogeneous fault properties and static and dynamic stresses decaying away from the rupture. The systematic recurrence of tremor demonstrated here suggests the potential to monitor detailed time-varying deformation on this portion of the deep San Andreas fault, deformation which unsteadily loads the shallower zone that last ruptured in the 1857 magnitude-7.9 Fort Tejon earthquake[8].

Earthquakes on the San Andreas fault mostly range between depths of 2 and 15 km and provide information about the location and style of deformation of the fault in this upper-crustal 'seismogenic' zone. Beyond the maximum depth of earthquakes, however, relatively little is known about the character of the fault. While some have proposed that the San Andreas and other faults may evolve into broadly distributed zones of deformation beneath the seismogenic layer[9], recent observations of deep tremor and slow slip suggest that faults can remain localized well below the down-dip limit of earthquakes[10].

Deep tremor was first observed in the subduction zones of southwest Japan[1] and Cascadia[11]. In these locations, the majority of tremor is generated in relatively large bursts of concentrated activity, often accompanied by geodetically detectible slow slip. In southwest Japan, these bursts typically last several days and occur at periods of 3–6 months[12]. By comparison, Cascadia events tend to be larger in area, longer in duration, and less frequent, with typical periodicities of 10–19 months, depending on the location of events along the margin[13].

Tremor has also been identified beneath the strike-slip San Andreas fault near Parkfield, California. This tremor exhibits many of the same characteristics as subduction zone tremor, including a dominant frequency content of ~2–8 Hz (ref. 5), apparent location on the deep extension of the fault, and waveforms consisting of repeated similar events[4]. In addition, like tremor in Nankai and Cascadia, San Andreas fault tremor is triggered by very small stresses imparted by teleseismic waves[14–16] and tidal fluctuations[17]. Tremor locations aligned with fault strike[4] and triggering by tidally induced right lateral shear stress[17] strongly suggest that San Andreas fault tremor is generated by tectonically driven slip on the deep fault, as has been argued for tremor in Japan[2,18] and Cascadia[3]. Despite the many similarities to subduction zone tremor, no accompanying geodetic signature has yet been detected near Parkfield[19], probably owing to the relatively small spatial dimension and short recurrence times of activity in this area.

As in southwest Japan[18], tremor beneath the San Andreas fault is composed of an overlapping sequence of individual events[4], which have been termed low-frequency earthquakes[20]. While semi-continuous activity and low amplitudes often prevent identification of the P and S wave arrivals that are generally used to locate earthquakes, repeated activity from the same patch of the fault can be identified very effectively using cross-correlation in a multi-channel matched filter[21].

Figure 1 shows estimated locations for the suite of 21 different low-frequency earthquakes from ref. 6. As described in that work, these low-frequency earthquakes are used as template events and are then scanned through continuous borehole seismic data from the Parkfield High Resolution Seismic Network (HRSN) from mid-2001 to the end of 2008, with similarity measured as the sum of the correlation coefficients across all channels[18]. The set of events resembling each template is considered an event family.

This approach has several advantages over amplitude-based analysis of tremor[7], including the ability to identify short-duration tremor and low-amplitude tremor. Furthermore, because it relies on the shape and timing of the waveforms, rather than waveform envelopes, this method permits analysis on much shorter spatial and temporal scales, differentiating activity on many small patches of the deep fault. Similarly, this technique automatically differentiates between tremor and other seismic signals, such as earthquake aftershocks or cultural noise. Thus, there is no need to exclude the times immediately following significant earthquakes, when amplitude detection becomes impractical owing to the difficulty of distinguishing semi-continuous shallow aftershocks from deep fault tremor[7].

One of the striking results of this analysis is the constant motion of the tremor source. Figure 2 shows an example of an extensive migration episode, in which the tremor source propagates ~25 km northwest along fault strike over a period of 90 min. This gives an average migration rate of 17 km h^{-1} (4.6 m s^{-1}), but the migration rate appears to vary substantially, and local migration velocities are as high as 80 km h^{-1}, similar to migration rates observed in the up- and down-dip directions in southwest Japan[22]. Despite variations in propagation rate in this example, initial onsets of activity in each event

[1]US Geological Survey, 345 Middlefield Road, MS 977, Menlo Park, California 94025, USA.

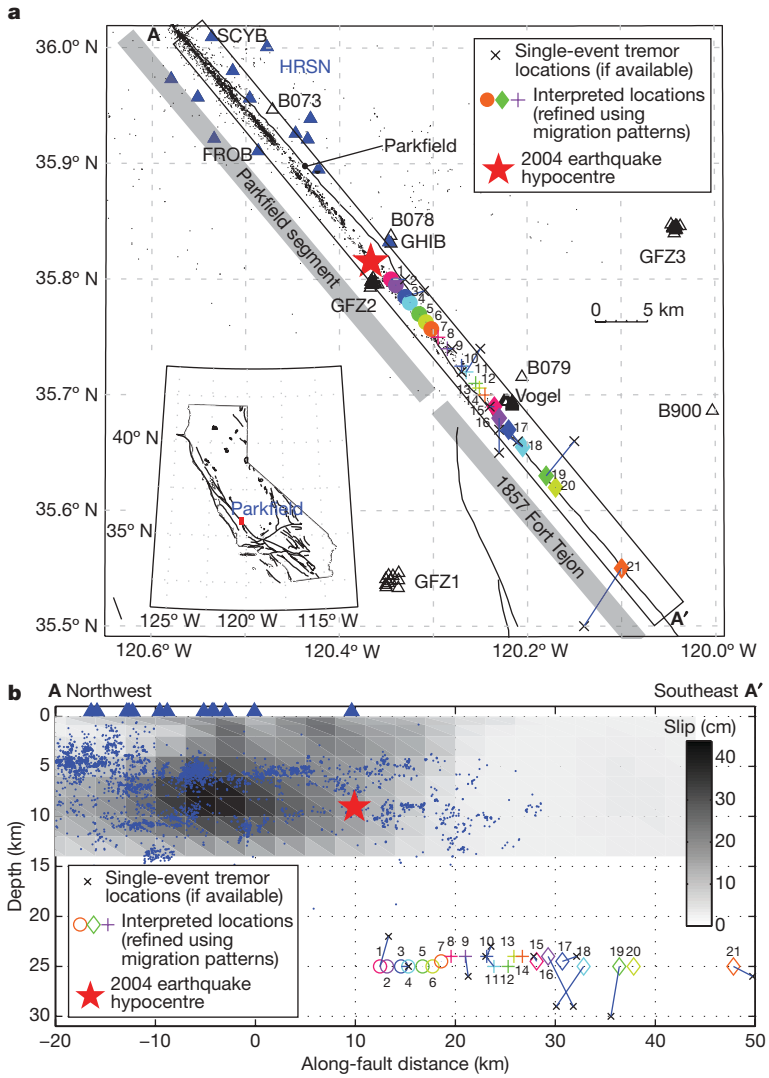

Figure 1 | Map and cross-section showing tremor locations. a, Map view. **b**, Cross-section. The red star shows the hypocentre of the 2004 earthquake. Coloured circle, plus, and diamond symbols show interpreted tremor event-family locations from ref. 6, derived from a combination of arrival time picks and migration patterns. Single-event travel-time-based locations for each family (when available) are shown as black 'x' symbols. Filled blue triangles are stations used in event detection, while black triangles are additional temporary and permanent stations used for template location. Small dots are relocated earthquakes[29]. Shaded grey regions denote the Parkfield segment, which last ruptured in 2004, and the northern end of the segment that last ruptured in the 1857 magnitude-7.9 Fort Tejon earthquake. The greyscale slip model in **b** includes coseismic slip and the first 230 days of afterslip from the 2004 Parkfield earthquake[30]. (Figure modified from ref. 6.)

family show a remarkably systematic progression to the northwest. Activity in a given event family often lingers after the initial front has passed, as seen in Fig. 2. Most San Andreas fault tremor migration episodes traverse shorter distances than in this example (5–10 km is common), yet persistent progressions between event families remain. An additional migration example is shown in Supplementary Fig. 3.

Along-strike tremor migration episodes, such as the one shown in Fig. 2, suggest that the fault exists as a continuous structure at the ~25 km depth of the tremors, near the ~26 km base of the crust in this area[23]. The nature of the fault between 15 and 24 km, however, is unknown, as this area is devoid of earthquakes and does not appear to generate appreciable tremor.

Despite migration episodes that sometimes encompass many event families, different families exhibit very different recurrence patterns, with typical recurrence periods ranging from a few days to a few months. Figure 3 shows cumulative events over time for three representative event families: one with large bursts of hundreds of events every few months, one with small bursts of several events every few days, and one with a hybrid pattern of large and small bursts.

Figure 4 summarizes this behaviour for all 21 families and demonstrates small-scale segmentation within the tremor zone, with groups of families showing coincident, or nearly coincident, bursts of activity. The highest overall level of tremor activity is observed during bursts lasting 1–3 days, recurring every few months. These can be seen in Fig. 4a as the apparent striping (bright bars) in families 8–11 and 13–17. Bursts of activity in these two zones often coincide closely in time, with activity in either zone preceding the other by 1–3 days. Occasionally, however, they become out-of-phase with one another, for example in mid-2006 (Figs 3a and 4a). Other event families typically exhibit small bursts of activity every few days, with varying degrees of regularity. For example, families 17–19 typically exhibit bursts of activity every 2–6 days (Fig. 4b and Supplementary Fig. 4); sometimes showing sympathetically increased activity along with large bursts at neighbouring families (Fig. 4b). This behaviour argues that different patches of the deep fault slip with corresponding variation in frequency, probably reflecting differences in the strength of the deep fault.

The semi-regularity of bursts at each family can be seen in Fig. 4b in the months preceding the 2004 Parkfield earthquake. This regularity suggests a model in which each burst of activity within a given family

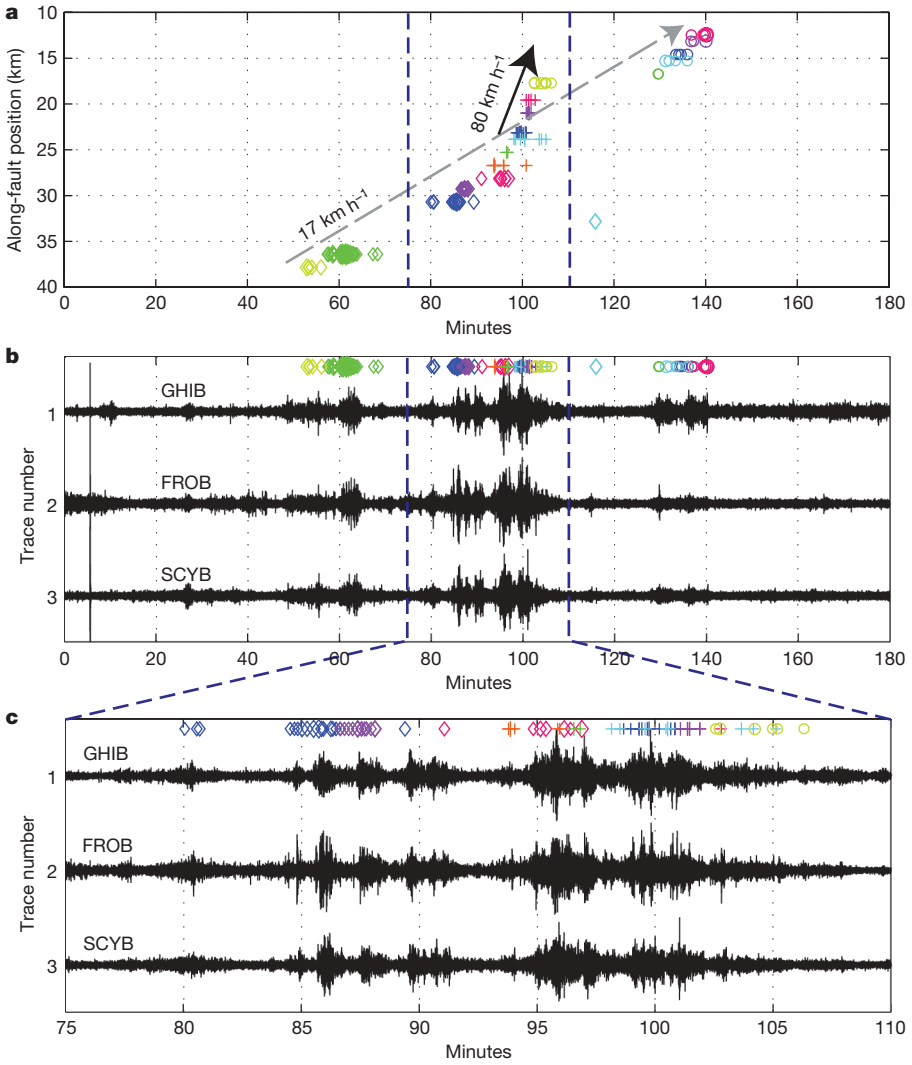

Figure 2 | Tremor migration. **a**, Example of an extended tremor migration episode, propagating ~25 km along fault strike over 90 min, from event family 20 northwest to event family 1. The average propagation rate in this episode is ~17 km, but local propagation rates vary substantially. Symbols are the same as in Fig. 1. This episode occurred on 26 October 2007 from 12:00–15:00 UTC (Coordinated Universal Time). **b**, Waveforms and event-family matches during the same period at three HRSN borehole stations (horizontal component). **c**, Zoomed view of the highest-amplitude (and fastest-migrating) portion of the sequence.

ruptures the same portion of the deep fault, releasing tectonic stress that is accumulated between bursts. If so, and I assume that slip averages ~3 cm yr^{-1}, I can estimate the amount of slip in each episode. Families with shorter return periods, for example 5 days, would average only 0.4 mm of slip in each burst. Assuming a 1 km radius dislocation (which should contain the members of a given family), the moment magnitude equivalent of such an event is 1.0 (assuming a shear modulus of 30 GPa), which will clearly fall below the detection thresholds of surface geodetic instruments. On the other hand, those families with the longest return periods display about three bursts a year, or ~1 cm of slip per event, and are somewhat more extensive, often 15 km along strike. Assuming a circular dislocation with a radius of 7.5 km, this would be equivalent to a moment magnitude of 4.8. Occurring at these depths (~25 km) over 2–3 days, such an event would probably still evade detection by current instrumentation[24], but might perhaps be observable by a long-baseline laser strainmeter recently installed in the area[25].

Tremor activity was strongly affected following the 2004 earthquake. The nature of the change, however, varies substantially within the tremor zone. The overall occurrence rates increased markedly for some families, but this effect mostly decayed with increasing distance from the earthquake rupture, as illustrated in cumulative event plots for three representative families in Fig. 3. On the other hand, the recurrence frequency of tremor bursts increased more broadly (Fig. 4b and Supplementary Figs 4 and 5), including some event families relatively distant from the rupture whose overall occurrence rates remained nearly constant, such as family 19 (rate is seen in Fig. 3; recurrence is shown in Fig. 4 and Supplementary Fig. 4). As this implies, the increased frequency of event bursts within a family was accompanied by a decrease in the number of events per burst (Figs 3 and 4), suggesting that the deep fault was temporarily weakened following the earthquake. This could imply that static stresses from the earthquake, which decay more quickly with distance, are driving the rate increase, while further-reaching dynamic stresses may temporarily weaken the fault. Although activity returned mostly back to the pre-earthquake pattern after a few months, occurrence rates in some families remained elevated through the end of the study period relative to their occurrence in the year preceding the 2004 earthquake, possibly reflecting an extended post-seismic deformation transient in the lower crust and/or uppermost mantle.

Although growing evidence supports deep fault shear failure as the basic mechanism of tremor, questions remain regarding physical conditions that control the spatial distribution of tremor. Tidal[17] and teleseismic[14–16] triggering of tremor imply that the deep fault is extremely sensitive to small stress perturbations, suggesting the presence of high (near-lithostatic) fluid pressure in the fault zone at these depths. If so,

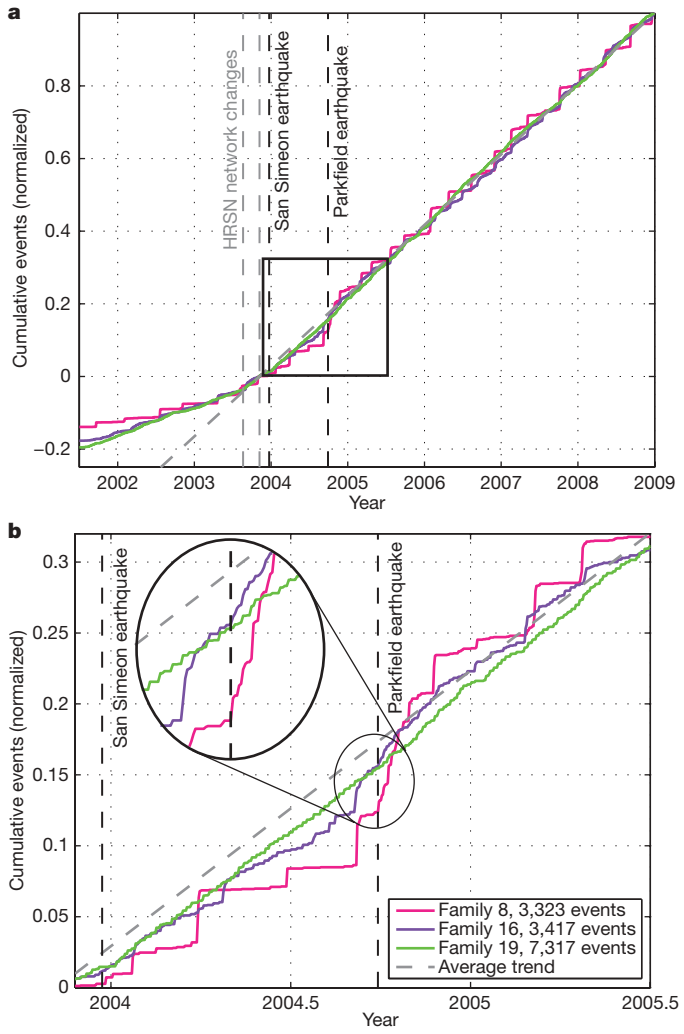

Figure 3 | Event-family recurrence styles. **a**, Cumulative events with time for three event families with different recurrence patterns. Family 8 (red) exhibits bursts containing many events every few months, while family 19 (green) exhibits smaller bursts every few days. Family 16 (purple) shows a hybrid behaviour of small bursts every few days and a larger burst every few months. Cumulative events are normalized to one between 6 November 2003 (the time of station operational changes) and 31 December 2008. Actual numbers of events are given in the legend. **b**, Zoomed view of **a**, with inset showing details of activity around the Parkfield earthquake, including small frequent bursts in family 19 (green). Notice that bursts in families 8 and 16 are often, but not always, concurrent, suggesting that these patches of the fault can rupture either together or separately.

the fluid source beneath the San Andreas fault is less obvious than in subduction zones, where slab dehydration is expected beneath the tremor zone. Nevertheless, many potential sources of fluid exist. Although a fossil slab may provide water beneath the San Andreas fault[26], the limited spatial extent of the San Andreas fault tremor argues for a more local control. Subducted sediments proposed to exist near the tremor zone[27] might provide a local source of fluids, as would serpentinite or fluid-saturated schist, which have been suggested to exist here on the basis of a receiver function study in this area[23]. High fluid pressures may make the fault extremely weak, possibly permitting patches of the deep fault to deform by brittle rather than ductile failure, even as temperatures approach 600 °C (ref. 28).

Tremor in this area provides an opportunity to examine the relationship between deep fault slip and earthquake occurrence. Whether or not a change in tremor activity might portend a future earthquake rupture is unknown, but high-resolution analysis of tremor provides a new ability to monitor temporal and spatial variations in deformation that might otherwise be concealed. Of particular current interest is tremor activity beneath the segment of the San Andreas fault south of Parkfield, a currently locked portion of the fault that last ruptured in the magnitude-7.9 Fort Tejon earthquake[8]. Although relatively subtle, changes in tremor migration patterns may have signalled accelerated deep fault slip in the three months leading up to the 2004 earthquake[6]. The marked changes in tremor activity following the 2004 earthquake appear to reflect the effects of static and dynamic

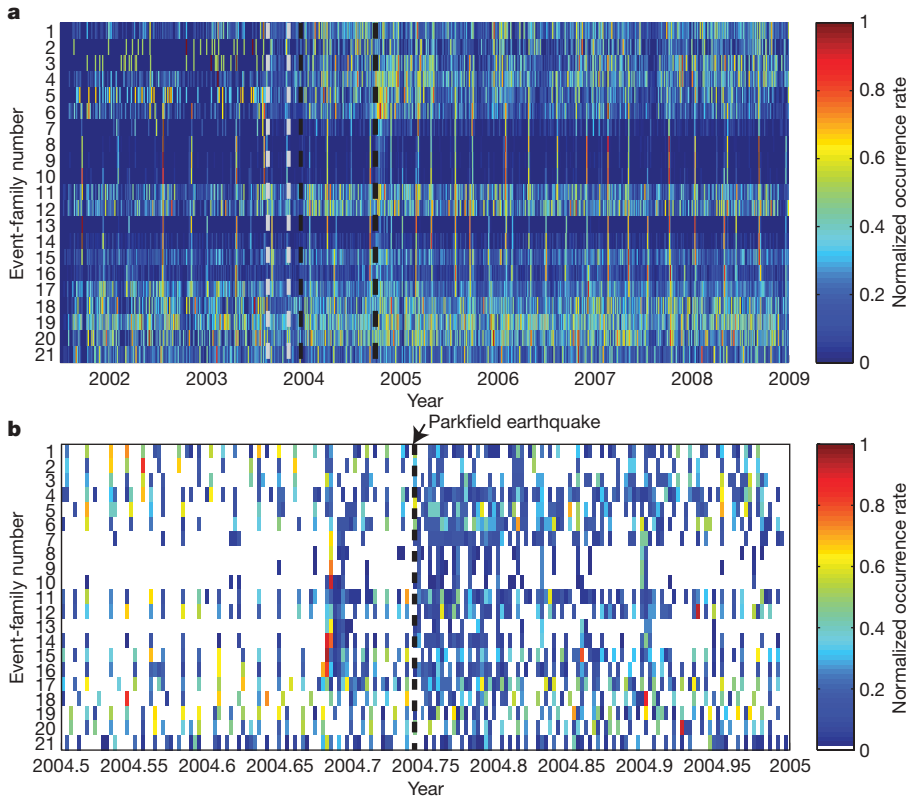

Figure 4 | Recurrence patterns for 21 event families. **a**, Number of events in a moving five-day window for each family from mid-2001 to the end of 2008, normalized by the maximum over this period. Events are ordered from northwest (top) to southeast (bottom), with the numbers corresponding to those in Fig. 1. Grey dashed lines in late 2003 indicate times of operational changes to HRSN stations. Black dashed lines indicate the times of San Simeon (22 December 2003) and Parkfield (28 September 2004) earthquakes. Normalization is performed separately before and after 20 August 2003, when the first changes to HRSN operational parameters were made. **b**, Events per day (rather than the five-day window of **a**) for each event family for the second half of 2004, bracketing the Parkfield earthquake. Event numbers are normalized by the maximum from 2001–2008 for each family. Notice the pronounced increase in event frequency for nearly all families following the earthquake. While bursts become more frequent, individual bursts contain fewer events, as indicated by the colours.

stresses imparted by the earthquake, demonstrating its relatively far-reaching influence on ongoing deep fault deformation.

METHODS SUMMARY

The event families and detected catalogue used here were introduced by ref. 6, supporting results describing possible changes in tremor activity preceding the 2004 magnitude-6.0 Parkfield earthquake. This processing consists of three main steps: template event selection, template event location and event detection. Template events are typically selected as relatively impulsive events within tremor in the continuous seismic data. When possible, the location is first estimated using compressional (P) and shear (S) wave arrival time picks for these events (Supplementary Table 1). Persistent migration patterns between event families suggest close spatial relationships and make it possible to refine these locations as well as to estimate locations of events for which phase arrivals are not sufficiently clear[6].

Additional events similar to each template event are detected by cross-correlating the template waveforms with the continuous data stream. Each waveform template consists of 6 s of the three-component waveform at each station, with time delays applied to approximately match the S-wave propagation across the network[18,22]. An example template is shown in Supplementary Fig. 1. This waveform template is then scanned through the continuous data with cross-correlations calculated every 0.05 s, with the time delays of the original template preserved. Similarity is measured by the correlation coefficient sum across all channels and stations of the network. For maximum consistency over time, I used the 25 channels of data from the HRSN network that operated most consistently over the study period and apply a fixed correlation sum threshold of 4.0.

Full Methods and any associated references are available in the online version of the paper at www.nature.com/nature.

Received 29 July; accepted 7 December 2009.

1. Obara, K. Nonvolcanic deep tremor associated with subduction in southwest Japan. *Science* **296,** 1679–1681 (2002).
2. Ide, S., Shelly, D. R. & Beroza, G. C. Mechanism of deep low frequency earthquakes: further evidence that deep non-volcanic tremor is generated by shear slip on the plate interface. *Geophys. Res. Lett.* **34,** L03308, doi:10.1029/2006GL028890 (2007).
3. Wech, A. G. & Creager, K. C. Cascadia tremor polarization evidence for plate interface slip. *Geophys. Res. Lett.* **34,** L22306, doi:10.1029/2007GL031167 (2007).
4. Shelly, D. R. *et al.* Precise location of San Andreas fault tremors near Cholame, California using seismometer clusters: slip on the deep extension of the fault? *Geophys. Res. Lett.* **36,** L01303, doi:10.1029/2008GL036367 (2009).
5. Nadeau, R. M. & Dolenc, D. Nonvolcanic tremors deep beneath the San Andreas fault. *Science* 307, 389, doi:10.1126/science.1107142 (2005); published online 9 December 2004.
6. Shelly, D. R. Possible deep fault slip preceding the 2004 Parkfield earthquake, inferred from detailed observations of tectonic tremor. *Geophys. Res. Lett.* **36,** L17318, doi:10.1029/2009GL039589 (2009).
7. Nadeau, R. M. & Guilhem, A. Nonvolcanic tremor evolution and the San Simeon and Parkfield, California earthquakes. *Science* **325,** 191–193 (2009).
8. Sieh, K. E. Central California foreshocks of the great 1857 earthquake. *Bull. Seismol. Soc. Am.* **68,** 1731–1749 (1978).
9. Page, B. M., Coleman, R. G. & Thompson, G. A. Overview: Late Cenozoic tectonics of the central and southern coast ranges of California. *Geol. Soc. Am. Bull.* **110,** 846–876 (1998).
10. Rubinstein, J. L., Shelly, D. R. & Ellsworth, W. L. in *New Frontiers in Integrated Solid Earth Science, International Year of Planet Earth* 287–314 (Springer, doi:10.1007/978-90-481-2737-5_8, 2010).
11. Rogers, G. & Dragert, H. Episodic tremor and slip on the Cascadia subduction zone: the chatter of silent slip. *Science* **300,** 1942–1943 (2003).
12. Obara, K. & Hirose, H. Non-volcanic deep low-frequency tremors accompanying slow slips in the southwest Japan subduction zone. *Tectonophysics* **417,** 33–51 (2006).
13. Brudzinski, M. R. & Allen, R. M. Segmentation in episodic tremor and slip all along Cascadia. *Geology* **35,** 907–910 (2007).
14. Gomberg, J. *et al.* Widespread triggering on non-volcanic tremor in California. *Science* **319,** 713 (2008).
15. Peng, Z. *et al.* Strong tremor near Parkfield, CA excited by the 2002 Denali earthquake. *Geophys. Res. Lett.* **35,** doi:10.1029/2008GL036080 (2008).
16. Peng, Z., Vidale, J. E., Wech, A., Nadeau, R. M. & Creager, K. M. Remote triggering of tremor around the Parkfield section of the San Andreas fault. *J. Geophys. Res.* **114,** B00A06, doi:10.1029/2008JB006049 (2009).
17. Thomas, A., Nadeau, R. M. & Bürgmann, R. Tremor-tide correlations and near-lithostatic pore pressure on the deep San Andreas fault. *Nature* **462,** 1048–1051 (2009).
18. Shelly, D. R., Beroza, G. C. & Ide, S. Non-volcanic tremor and low frequency earthquake swarms. *Nature* **446,** 305–307 (2007).
19. Johnston, M. J. S., Borcherdt, R. D., Linde, A. T. & Gladwin, M. T. Continuous borehole strain and pore pressure in the near field of the 28 September 2004 M 6.0 Parkfield, California, earthquake: implications for nucleation, fault response, earthquake prediction, and tremor. *Bull. Seismol. Soc. Am.* **96,** doi:10.1785/0120050822 (2006).
20. Katsumata, A. & Kamaya, N. Low-frequency continuous tremor around the Moho discontinuity away from volcanoes in the southwest Japan. *Geophys. Res. Lett.* **30,** doi:10.1029/2002GL015981 (2003).
21. Gibbons, S. J. & Ringdal, F. The detection of low magnitude seismic events using array-based waveform correlation. *Geophys. J. Int.* **165,** 149–166 (2006).
22. Shelly, D. R., Beroza, G. C. & Ide, S. Complex evolution of transient slip derived from precise tremor locations in western Shikoku, Japan. *Geochem. Geophys. Geosyst.* **8,** Q10014, doi:10.1029/2007GC001640 (2007).
23. Ozacar, A. A. & Zandt, G. Crustal structure and seismic anisotropy near the San Andreas fault at Parkfield, California. *Geophys. J. Int.* **178,** 1098–1104 (2009).
24. Smith, E. F. & Gomberg, J. A search in strainmeter data for slow slip associated with triggered and ambient tremor near Parkfield, California. *J. Geophys. Res.* doi:10.1029/2008JB005848 (in the press).
25. Agnew, D. C. & Wyatt, F. K. Long-base laser strainmeters: a review. ⟨http://repositories.cdlib.org/sio/techreport/2/⟩ (SIO Technical Report, Scripps Institution of Oceanography, 2003).
26. Kirby, S., Wang, K. & Brocher, T. A possible deep, long-term source for water in the northern San Andreas fault system: a ghost of Cascadia subduction past? *Eos* **83,** (Fall Meet. Suppl.) abstract S22B–1038 (2002).
27. Trehu, A. M. & Wheeler, W. H. Possible evidence for subducted sedimentary materials beneath central California. *Geology* **15,** 254–258 (1987).
28. Sass, J. H. *et al.* Thermal regime of the San Andreas fault near Parkfield, California. *J. Geophys. Res.* **102,** 27575–27585 (1997).
29. Thurber, C. *et al.* Three-dimensional compressional wavespeed model, earthquake relocations, and focal mechanisms for the Parkfield, California, region. *Bull. Seismol. Soc. Am.* **96,** S38–S49, doi:10.1785/0120050825 (2006).
30. Murray, J. & Langbein, J. Slip on the San Andreas fault at Parkfield, California, over two earthquake cycles, and the implications for seismic hazard. *Bull. Seismol. Soc. Am.* **96,** S283–S303, doi:10.1785/0120050820 (2006).

Supplementary Information is linked to the online version of the paper at www.nature.com/nature.

Acknowledgements I thank T. Ryberg and C. Haberland for sharing data from temporary arrays GFZ1, GFZ2 and GFZ3. G. Fuis assisted with permitting and installation of these stations and instruments were provided by GIPP of GFZ. W. Ellsworth and J. Murphy installed temporary stations at the Vogel site. I thank R. Nadeau for sharing his tremor catalogue. The HRSN is operated by UC-Berkeley, and seismic data was provided through the NCEDC. I thank J. Vidale, J. Hardebeck and J. Gomberg for reviewing various forms of this manuscript.

Author Information Reprints and permissions information is available at www.nature.com/reprints. The author declares no competing financial interests. Correspondence and requests for materials should be addressed to the author (dshelly@usgs.gov).

METHODS

The event families and detected catalogue used here were introduced by ref. 6, in support of work describing possible changes in tremor activity preceding the 2004 magnitude-6.0 Parkfield earthquake. This processing consists of three main steps: template event selection, template event location and event detection. For convenience, these steps are summarized below.

Selection of waveform templates. The waveform templates used in this study are those used by ref. 6 and are selected from the continuous data. Templates are identified largely by a process of trial and error. To find a new template, I looked for tremor not matched by any current templates. Within this unmatched tremor, I attempted to select relatively strong and isolated events as templates.

To compare tremor rates over time, I must consider the possibility that tremor waveforms may change over periods of years, either due to a change in the source or a change in the earth (for example, changes induced by the San Simeon or Parkfield earthquakes). To test this possibility, I compared the event detection rates from similar waveform templates recorded during different years. I found no significant change over the 7.5 years of this study, and in general used the template that appears to have the highest signal-to-noise ratio.

Template event location. Tremor locations shown in Fig. 1 from ref. 6 are derived from a hybrid process. Whenever possible, I obtained an absolute location for each template event based upon P and S wave arrival times of a low-frequency earthquake with a good signal-to-noise ratio at permanent and temporary stations. These additional stations, shown as open black triangles in Fig. 1a, helped greatly to constrain the locations. To evaluate the range of possible hypocentres and their corresponding residuals, the locations were performed by a grid search (Supplementary Fig. 2) using a one-dimensional approximation to the velocity model of ref. 29 near this location, with a V_P/V_S ratio of 1.78 (where V_P and V_S are the velocities of the P- and S-waves), as done by ref. 4. Uncertainty in these locations was approximately ± 4 km in horizontal and vertical positions. Owing to station distribution, uncertainties tended to be slightly smaller for the northerly tremors (closer to Parkfield) and slightly larger for the southernmost tremors, for example, families 18–21. I obtained absolute locations for 11 of the 21 template events shown in Fig. 1; these coordinates are given in Supplementary Table 1 of ref. 6. Phase arrival time picks (P and S waves) for these events are given here in Supplementary Table 1. Using the absolute locations as a framework, I then refined these locations by observing persistent patterns of migration between event families. For example, if I consistently observed migration from family A to family B to family C, or the reverse of this, I inferred that family B is located between families A and C. I also used migration patterns to infer event locations for which no absolute location can be determined, owing to insufficient identifiable P and S wave arrivals. Because the depth range of single-event locations (22–30 km) can nearly be explained by uncertainty, I plotted all events in the range of 24–25 km, which represents an average depth of the best-constrained events. Small perturbations are plotted to help explain migration patterns and differences in recurrence behaviour, but these differences are neither well constrained nor critical to the analysis presented here.

Event detection. I used the detection catalogue introduced by ref. 6, obtained by a procedure adapted from previous work[18,22]. The waveform template consists of 6 s of the three-component waveform at each station, with time delays applied to approximately match the S-wave propagation across the network. An example template is shown in Supplementary Fig. 1. I cross-correlated each waveform template with the continuous data stream, preserving the time lags across stations. I used data of 20 samples per second, bandpass filtered at 2–8 Hz, and performed the cross-correlation at lag increments of one sample. Similarity is then measured by the correlation sum across all channels and stations of the network. Finally, a threshold was applied. For maximum consistency over time, I used a fixed correlation sum threshold of 4.0 for the 25 selected channels, with a maximum of one event every 4 s.

Comparison with a tremor catalogue determined by amplitude and duration (R. Nadeau, personal communication, 2008) shows good agreement, although I identified many weak or short-duration tremor episodes missing from the amplitude-based catalogue. Specifically, I compared my results with a catalogue of well-located events south of Parkfield for 2006–2007 (R. Nadeau, personal communication, 2008). Although additional templates would be required to match all tremor, I detected at least one event within 99% (305/308) of bursts identified by amplitude and duration. Individual template events match between several hundred and several thousand events over the 7.5 years examined here. Tremor also occurs along the San Andreas fault north of Parkfield[7] and additional template events would be necessary to detect this tremor as well as for additional tremor south of Parkfield.

Stations and components used for consistent detection. To compare tremor rates over time, I used the following stations and channels, which operated most consistently during the study period (STATION.CHANNELS): EADB.123, FROB.123, JCSB.123, LCCB.23, MMNB.3, RMNB.12, SCYB.123, SMNB.123, VCAB.123, GHIB.13 (two-component non-functional at GHIB). The following stations and channels were not used: CCRB.123, JCNB.123, LCCB.1, MMNB.12, RMNB.3, VARB.123 (instrument replaced at new depth in August 2003 at VARB).

Stations used for template event locations. Although the HRSN stations provide optimal long-term tremor detection capability, their concentrated distribution offset from the tremor activity does not provide good location ability. Therefore, I employed additional stations (shown in Fig. 1) to constrain the data. In particular, I used four temporary arrays of ten stations each (GFZ1, GFZ2, GFZ3, Vogel)[4] and six individual three-component stations from the Plate Boundary Observatory and HRSN (B079, B078, B900, B073, GHIB, FROB). Two additional stations from the Southern California Seismic Network (SMM and PHL) were used to help locate the southernmost event family (family 21).